Supplementary Information

The structural function of nestin in cell body softening is correlated with cancer cell metastasis

Ayana Yamagishi, Moe Susaki, Yuta Takano, Mei Mizusawa, Mari Mishima, Masumi Iijima, Shun'ichi Kuroda, Tomoko Okada, Chikashi Nakamura*

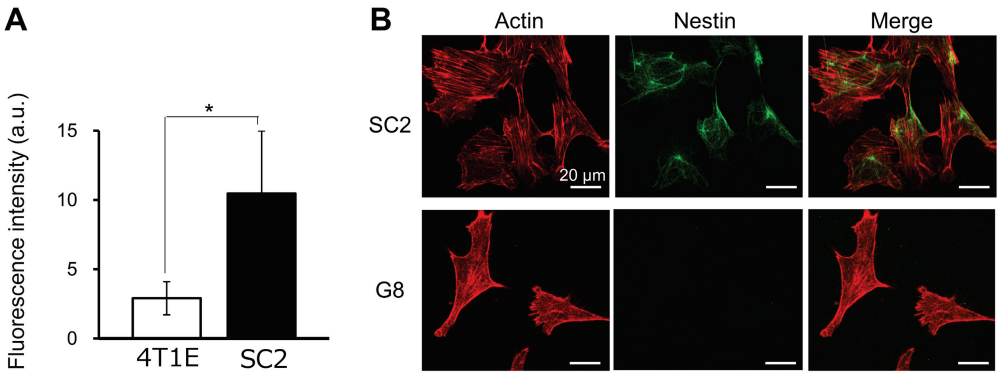

Figure S1. Nestin knockout in the FP10SC2 mouse breast cancer cell line, which highly expresses nestin. (A) Expression levels of nestin in 4T1E and FP10SC2 cells. Fluorescence intensity in immunostained images was measured using ImageJ software. (B) Immunostaining of actin (red) and nestin (green) in FP10SC2 and nestin knockout SNKOG8 cells.

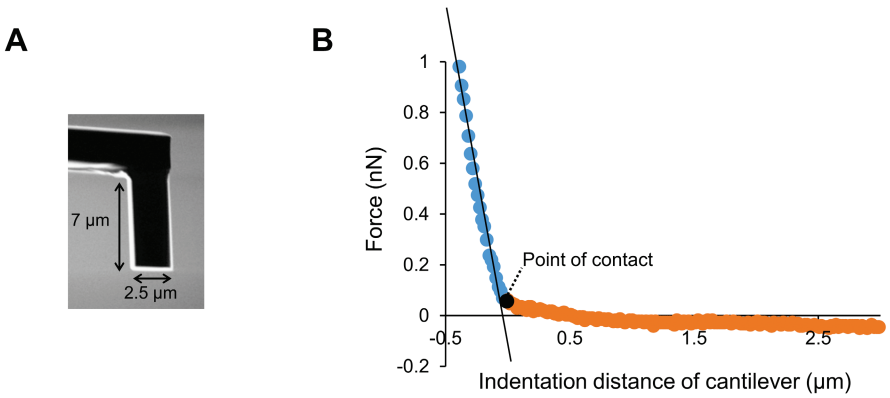

Figure S2. Stiffness of cells, as measured by cylindrical cantilever insertion. (A) Scanning ion microscopy (SIM) image of a cylindrical cantilever, which was obtained after the fabrication using a focused ion beam. (B) Force-indentation curve generated during the process of indentation of the cylindrical cantilever into an FP10SC2 cell.

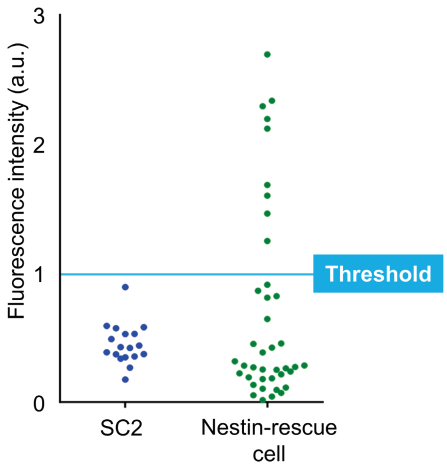

Figure S3. Distribution of nestin expression level in nestin-rescue SNKG8 cell. To remove nestin-overexpression cells, we set the threshold value which was the average fluorescent intensity derived from nestin plus four standard deviations of positive control, FP10SC2.

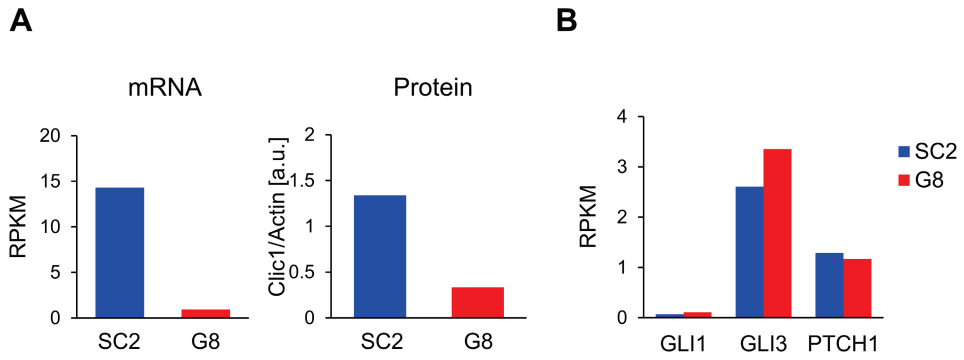

Figure S4. RNA-seq analysis for mRNA expression in FP10SC2 and SNKG8. (A) Expression of chloride intracellular channel 1 (Clic1) in FP10SC2 and SNKG8 cells. Left panel shows reads per kilobase of exon per million mapped reads (RPKM) value of Clic1 mRNA analyzed by RNA-seq and right one shows Clic1 protein expression level evaluated by dot blotting. The results were normalized to actin protein expression. (B) RPKM values of genes related to hedgehog signal pathway.

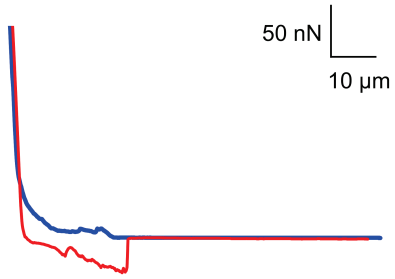

Figure S5. Tensile test of nestin in FP10SC2 cells using a nanoneedle with immobilized anti-nestin antibodies. Force curves obtained by needle insertion and retraction processes are shown in blue and red, respectively. The slope of the force curve was moderate, similar to that observed for vimentin.

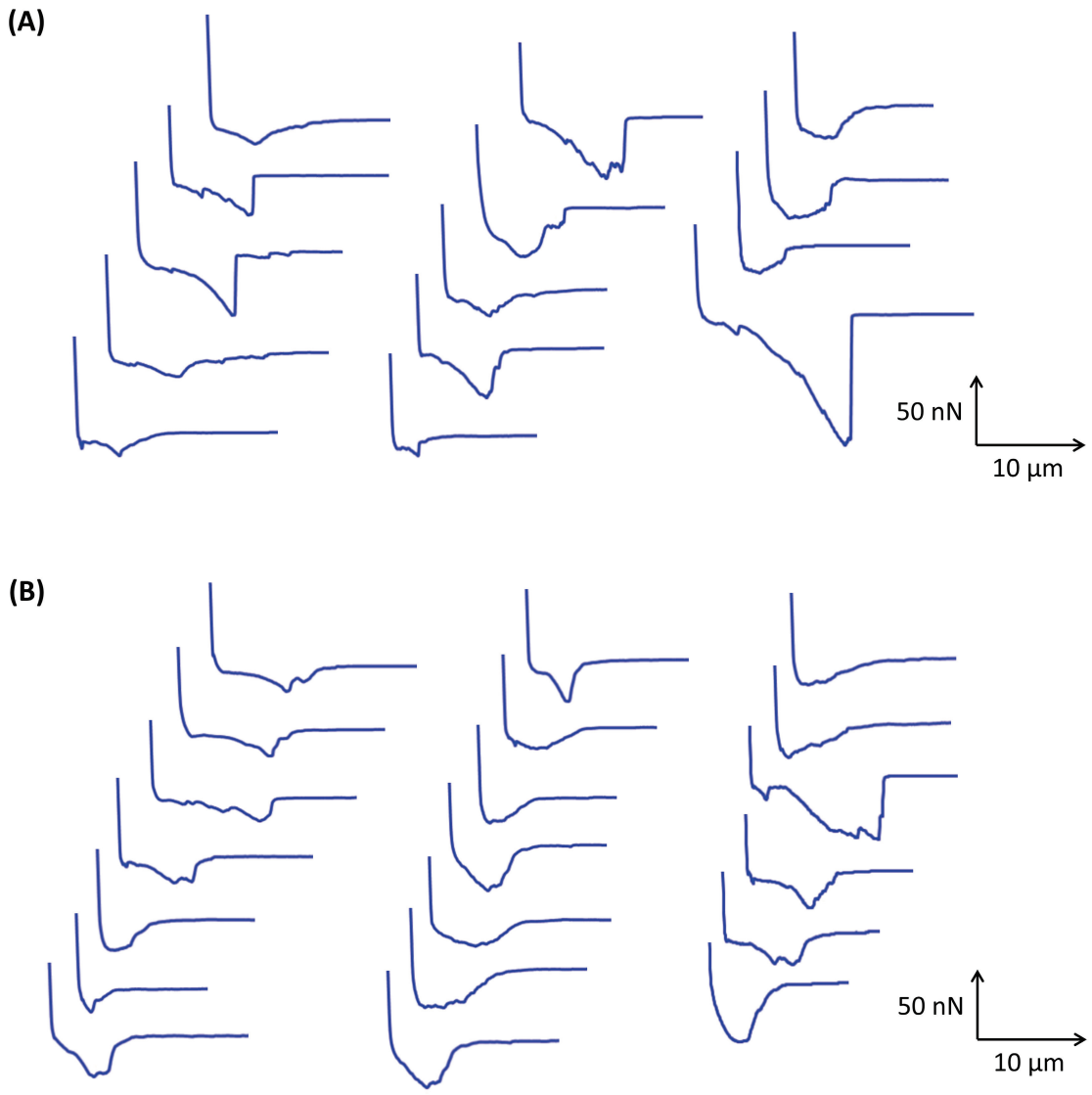

Figure S6. Force curves obtained by tensile testing of vimentin in FP10SC2 (A) and SNKG8 cells (B). The curves reflect the retraction process of an anti-vimentin antibody-modified nanoneedle after insertion into a cell.

Table S1. List of top 20 up- and down-regulated genes when comparing FP10SC2 to nestin knockout cell

Regulation	Accession No.	Annotation	FP10SC2 RPKMs	Nestin KO RPKMs	Log2 fold change
Up-regulated	NM_172685.3	Solute carrier family 25 (mitochondrial carrier phosphate carrier) member 24	0.0092	0.8923	6.60
	NM_007883.3	Desmoglein-2	0.0323	1.8653	5.85
	NM_025645.2	Small nuclear ribonucleoprotein 40 (U5)	0.0195	1.0024	5.68
	NM_019693.3	DEAD (Asp-Glu-Ala-Asp) box polypeptide 39B	0.1430	3.7664	4.72
	NM_009597.1	Acid-sensing (proton-gated) ion channel 1	0.0248	0.6280	4.66
	NM_177782.3	Phosphatidylinositol-3 4 5-trisphosphate-dependent Rac exchange factor 1	0.0619	1.1775	4.25
	NM_026688.2	NADH dehydrogenase (ubiquinone) Fe-S protein 3	0.0992	1.7874	4.17
	NM_011950.2	Mitogen-activated protein kinase 13	0.0896	1.3952	3.96
	NM_009994.1	Cytochrome P450 family 1 subfamily b polypeptide 1	0.0546	0.7275	3.74
	NM_194344.2	SH3 domain and tetratricopeptide repeats 1	0.0957	1.0580	3.47
	NM_175314.3	Disintegrin-like and metallopeptidase (reprolysin type) with thrombospondin type 1 motif 9	0.0515	0.5520	3.42
	NM_001085371.1	SPEG complex locus	0.0824	0.8807	3.42
	NM_016844.2	Ribosomal protein S28	2.8435	29.8666	3.39
	NM_177068.4	Olfactomedin-like 2B	0.1205	1.1501	3.25
	NM_011347.2	Selectin platelet	0.1356	1.2839	3.24
	NM_178929.4	Kazal-type serine peptidase inhibitor domain 1	0.1126	1.0524	3.22
	NM_010357.3	Glutathione S-transferase alpha 4	0.6166	4.8751	2.98
	NM_054041.2	Anthrax toxin receptor 1	0.0945	0.7249	2.94
	XM_006527345.3	MAM domain containing 2	0.0832	0.6094	2.87
	NM_001291928.1	Adenosine A1 receptor	0.1361	0.9908	2.86

Down-regulated	NM_001017427.1	RAS and EF hand domain containing	0.6418	0.0824	-2.96
	NM_029306.3	RIKEN cDNA 1700012B09 gene	1.4008	0.1656	-3.08
	NM_010680.1	Laminin alpha 3	2.2123	0.2065	-3.42
	NM_175662.2	Histone cluster 2 H2ac	1.3286	0.1217	-3.45
	NM_011495.2	Polo-like kinase 4	0.6223	0.0562	-3.47
	NM_057171.2	BCL2-associated athanogene 6	0.8381	0.0738	-3.51
	NM_027435.2	ATPase family AAA domain containing 2	1.5318	0.1052	-3.86
	NM_023043.3	Prion protein dublet	1.6141	0.1075	-3.91
	NM_033444.2	Chloride intracellular channel 1	14.3241	0.9337	-3.94
	NM_001143689.1	Histocompatibility 2 Q region locus 4	1.0384	0.0582	-4.16
	NM_020603.2	WD repeat domain 46	1.4223	0.0790	-4.17
	NM_018815.2	Nucleoporin 210	1.3125	0.0567	-4.53
	NM_001289490.1	O-acyl-ADP-ribose deacylase 1	0.5281	0.0210	-4.65
	NM_017368.3	CUGBP Elav-like family member 1	1.5554	0.0589	-4.72
	NM_001347228.1	Protein-L-isoaspartate (D-aspartate) O-methyltransferase 1	0.9219	0.0332	-4.79
	NM_145959.3	Family with sequence similarity 91 member A1	2.3119	0.0659	-5.13
	NM_011432.2	U1 small nuclear ribonucleoprotein C	8.5791	0.2245	-5.26
	NM_023476.3	Tubulointerstitial nephritis antigen-like 1	3.8583	0.0952	-5.34
	NM_027196.4	Polymerase (DNA-directed) delta 4	2.3004	0.0310	-6.21
	NM_001168470.1	ER membrane protein complex subunit 6	2.1510	0.0203	-6.73

Log2 fold change values were calculated from a following formula, $\log_2$ (Nestin KO RPKM / FP10SC2 RPKM).

Movie S1. 3D movie of the interaction between vimentin and actin filament in a SNKG8 cell, detected by immunofluorescence microscopy during proximity ligation assay analysis. The movie was reconstructed from images taken at 0.1-μm distances throughout the cell by confocal laser-scanning microscopy.